Electronic Supplementary Information (ESI)

Thermodynamic Modelling of Acidic Collagenous Solutions: From Free Energy Contributions to Phase Diagrams

Sayyed Ahmad Khadem and Alejandro D. Rey*

Department of Chemical Engineering, McGill University, 3610 University Street, Montreal, Quebec, H3A 0C5, Canada.

*To whom correspondence should be addressed. Tel.: + 1-514-398-4196. E-mail: alejandro.rey @mcgill.ca

Appendix A: Details of energy landscape derivation

The purpose of this appendix is to provide the mathematical details and intermediate steps used in deriving the energy landscape given in eqns. (8, 10, 11a, 15, 21a, 22a, 26 and 29a).

A.1. Impact of interchain interactions

The aim of this subsection is to elaborate the derivation of eqns. (8, 10, 11a). The common assumption about the orientation distribution function is its independency from the azimuthal angle (1-3) in spherical coordinates. Therefore, the $\mathbf{u}$ is variable with respect to only polar angle and $\psi(\mathbf{u}) = \psi(\theta)$.

According to Maier-Saupe theory (2, 4, 5), the averaged potential of orientation-dependent attractive interactions for i^{th} rod among the other macromolecules is given by eqn. (A.1.1) (2, 4-6).

$$\beta U_i^{MS} = -\beta U'^{MS} \upsilon_A S P_2(\cos\theta) \tag{A.1.1}$$

To obtain the corresponding energy, eqn. (A.1.1) needs to be substituted into eqn. (A.1.2a). Doing so, we get eqn. (A.1.2b), (6).

$$\beta E^{MS} = \frac{Z N_A}{2} \iint \beta U_i^{MS} \psi(\theta) \psi(\theta') d\Omega d\Omega' \tag{A.1.2a}$$

$$\beta E^{MS} = -\beta U'^{MS} \upsilon_A S \frac{Z N_A}{2} \int P_2(\cos\theta) \psi(\mathbf{u}) d\Omega \int \psi(\mathbf{u}') d\Omega' \tag{A.1.2b}$$

In eqn. (A.1.2b), the first integral indicates the definition of scaler order parameter, and the second integral is the normalization of distribution function that is equal to one (see eqns. (17-18)). Therefore, eqn. (A.1.2b) can be rewritten as eqn. (A.1.3).

$$\beta E^{MS}=-\beta U^{MS}\upsilon_A S^2 N_A \qquad (A.1.3)$$

Furthermore, $N_A=c_A V$ and for pure liquid crystals $V=\upsilon_A N_A$, we then write the contribution of orientation-dependent attractive interactions on the energy landscape as eqn. (A.1.4).

$$\frac{\beta E^{MS}}{N_A}=-\beta U^{MS} S^2 c_A \upsilon_A^2 \qquad (A.1.4)$$

It should be noticed that the eqn. (A.1.4) has been also used in the other studies (2, 7, 8). Now we turn to the modeling of mean-field potential for repulsion and twisting. When two rods are positively charge, the most stable configuration for them becomes orthogonal; see Fig. 1.

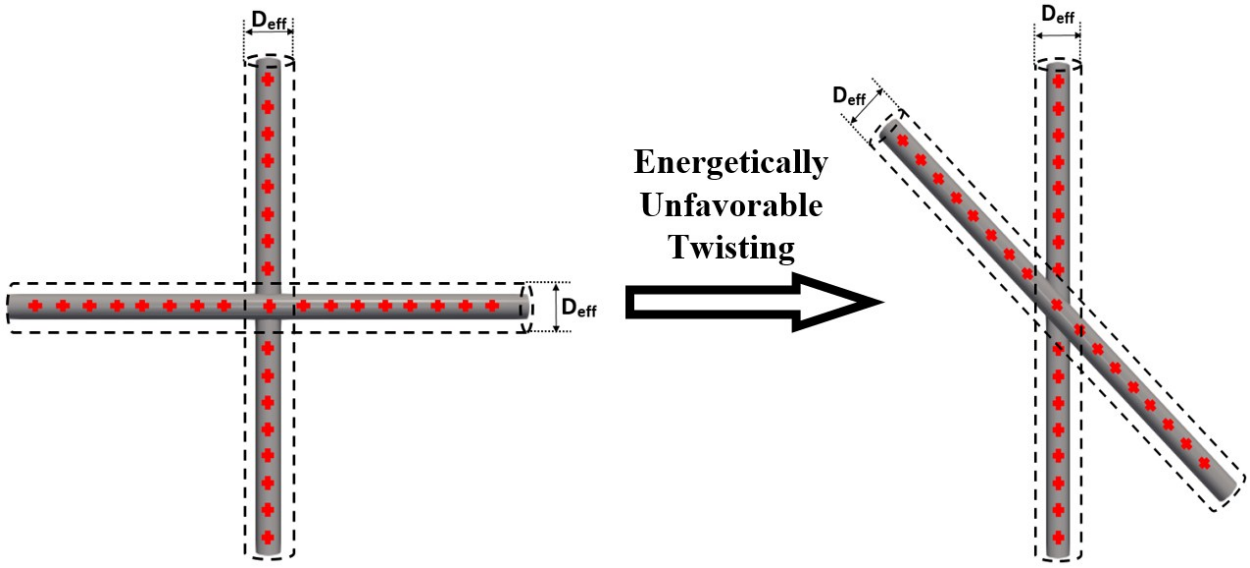

Fig. 1 : Phase ordering of two positively charged rods.

Phase ordering is thus energetically unfavorable process. To model this phenomenon, we use the Maier-Saupe potential with a positive sign (eq. (9)). Doing so dictates that the orientational ordering for charged rods gives rise to an increase in the free energy. Similarly, after taking the molecular average of the obtained mean-field potential (eqn. (A.1.2a)); the eqn. (10) of the article is obtained. Finally, the net of orientation-dependent intermolecular interactions reads:

$$M=\frac{\beta E^{MS}}{N_A}+\frac{\beta E^{elc}}{N_A}=\beta\left(U^{elc}-U^{MS}\right)S^2 c_A \upsilon_A^2 \qquad (A.1.5)$$

A.2. Impact of chirality

This subsection gives the detailed steps concerning the derivation of eqn. (15). The Mermin Frank energy for the macroscopic chirality, $E^{Cholesteric}$, the ideal equilibrium director, $\mathbf{n}$, and $\mathbf{Q}$-tensor are given by eqn. (A.2.1a-c), (9, 10).

$$E^{Cholesteric}=\frac{L_1}{2}\left(\nabla\times\mathbf{Q}+2q\mathbf{Q}\right)^2 \upsilon_A N_A \tag{A.2.1a}$$

$$\mathbf{Q}=S\left(\mathbf{nn}-\boldsymbol{\delta}/3\right) \tag{A.2.1b}$$

$$\mathbf{n}=\left[\cos(qz) \quad \sin(qz) \quad 0\right] \tag{A.2.1c}$$

Using the eqn. (A.2.1b), the $\nabla\times\mathbf{Q}$ reduces to $S\nabla\times\mathbf{nn}$. Second rank tensor of $\mathbf{nn}$ is constructed by eqn. (A.2.1c).

$$\mathbf{nn}=\begin{bmatrix} \cos^2(qz) & \sin(2qz)/2 & 0 \\ \sin(2qz)/2 & \sin^2(qz) & 0 \\ 0 & 0 & 0 \end{bmatrix} \tag{A.2.2}$$

Based on the Einstein notation, $\nabla\times\mathbf{nn}=\varepsilon_{ipq}\dfrac{\partial(\mathbf{nn})_{jq}}{\partial x_p}$ where ε_{ipq} is Levi-Civita function and x_p indicates spatial directions. Thus, using eqn. (A.2.2) leads to $\nabla\times\mathbf{nn}=0$ and eqn. (A.2.1a) reduces to eqn. (A.2.3).

$$E^{Cholesteric}=2L_1q^2\mathbf{Q}:\mathbf{Q} \tag{A.2.3}$$

Now we need to use eqn. (A.2.1b) for further simplification of eqn. (A.2.3).

$$\mathbf{Q}:\mathbf{Q}=S^2\left(\mathbf{nn}:\mathbf{nn}-\frac{1}{3}\mathbf{nn}:\boldsymbol{\delta}-\frac{1}{3}\boldsymbol{\delta}:\mathbf{nn}+\frac{1}{9}\boldsymbol{\delta}:\boldsymbol{\delta}\right) \tag{A.2.4}$$

The $\boldsymbol{\delta}=\mathbf{ii}+\mathbf{jj}+\mathbf{kk}$ where $\mathbf{i}$, $\mathbf{j}$ and $\mathbf{k}$ are unit vector in x, y and z directions, respectively. Hence, $\mathbf{nn}:\boldsymbol{\delta}=\mathbf{nn}:(\mathbf{ii}+\mathbf{jj}+\mathbf{kk})=\mathbf{nn}:\mathbf{ii}+\mathbf{nn}:\mathbf{jj}+\mathbf{nn}:\mathbf{kk}=(\mathbf{n}\cdot\mathbf{i})^2+(\mathbf{n}\cdot\mathbf{j})^2+(\mathbf{n}\cdot\mathbf{k})^2=\mathbf{n}\cdot\mathbf{n}=1$. In the similar way, $\boldsymbol{\delta}:\mathbf{nn}=\mathbf{nn}:\boldsymbol{\delta}=1$. Also, $\mathbf{nn}:\mathbf{nn}=(\mathbf{n}\cdot\mathbf{n})^2=1$ and $\boldsymbol{\delta}:\boldsymbol{\delta}=3$. We then get eqn. (A.2.5).

$$\mathbf{Q}:\mathbf{Q}=\frac{2}{3}S^2 \tag{A.2.5}$$

Now that $\mathbf{Q}:\mathbf{Q}$ is determined, also considering the assumptions $n_A^{eff}=L/D_{eff}$ and $\upsilon_i=a^3 n_i$ (2), the energy due to macroscopic chirality can be rearrange into eqn. (A.2.6).

$$\frac{\beta E^{Cholesteric}}{N_A}=\frac{32\pi^2}{3}\left(\frac{\xi}{p_0}\right)^2 S^2\frac{L}{D_{eff}} \tag{A.2.6}$$

where the nm-scale coherence (correlation) length is defined as $\xi=\sqrt{a^3 L_l \beta/2}$.

A.3. Finding optimal distribution function

This subsection aims to explain the intermediate steps in the derivation of the optimal normalized distribution function given by eqns. (21a, 22a). In this regard, we have to do the following optimization given in eqn. (A.3.1), (2).

$$\begin{cases}\text{minimize}: \dfrac{\delta F^s}{\delta\psi(\theta)} \\ \text{subject to}: \int\psi(\theta)d\Omega=1\end{cases} \tag{A.3.1}$$

$\frac{\delta F^s}{\delta\psi(\theta)}$ is the functional derivative of total free energy of system. This optimization can be transformed into nonlinear algebraic equations by the use of Euler-Lagrange multiplier, eqn. (A.3.2), (11):

$$\frac{\delta H}{\delta\psi(\theta)}=\frac{\delta F^s}{\delta\psi(\theta)}-\eta''\int\psi(\theta)d\Omega=0 \tag{A.3.2}$$

$\frac{\delta H}{\delta\psi(\theta)}$ and η'' are called the Hamiltonian function and Lagrange multiplier. Using eqn. (16) of the article, we reach eqn. (A.3.3a).

$$\frac{\delta H}{\delta\psi(\theta)}=\frac{N_A}{\beta}\left(\frac{\delta\sigma(\psi(\theta))}{\delta\psi(\theta)}+\bar{\upsilon}_{AA}c_A\frac{\delta\rho(\psi(\theta))}{\delta\psi(\theta)}+\left(Uc_A\upsilon_A^2+\frac{32\pi^2}{3}\left(\frac{\xi}{p_0}\right)^2\frac{L}{D_{eff}}\right)\frac{\delta S^2}{\delta\psi(\theta)}\right)$$
$$-\eta''\frac{\delta\int\psi(\theta)d\Omega}{\delta\psi(\theta)}=0 \tag{A.3.3a}$$

$$\frac{\delta\sigma(\psi(\theta))}{\delta\psi(\theta)}=2\pi\sin(\theta)\left(1+\ln(4\pi\psi(\theta))\right) \tag{A.3.3b}$$

$$\frac{\delta\rho(\psi(\theta))}{\delta\psi(\theta)} = 2\pi\sin(\theta)\frac{8}{\pi}\int\Gamma(\gamma)\psi(\theta')d\Omega' \tag{A.3.3c}$$

$$\frac{\delta S^2}{\delta\psi(\theta)} = 2S\frac{\delta S}{\delta\psi(\theta)} = 4\pi S\sin(\theta)P_2(\cos\theta) \tag{A.3.3d}$$

$$\frac{\delta\int\psi(\theta)d\Omega}{\delta\psi(\theta)} = 2\pi\sin(\theta) \tag{A.3.3e}$$

Substituting eqns. (A.3.3b-e) into eqn. (A.3.3a) gives the irreducible integral equation expressed in eqn. (19) of the article whereby the optimal distribution function, eqn. (21a) and eqn. (22a), can be obtained.

A.4. Derivation of mixing free energy

The objective of this subsection is to clarify the derivation of eqn. (26) in full detail. Because in the isotropic state $\sigma(\psi(\theta))=0$ and $\rho(\psi(\theta))=1$, and in the pure solution $c_A=(\upsilon_A)^{-1}$, the free energy of the pure components are expressed as eqns. (A.4.1a,b), (2, 12).

$$\beta F^s(N_A,0)=N_A\beta\mu_A^o-N_A+N_A\ln\upsilon-N_A\ln\upsilon_A+\frac{\bar{\upsilon}_{AA}N_A}{\upsilon_A} \tag{A.4.1a}$$

$$\beta F^s(0,N_I)=N_I\beta\mu_I^o-N_I+N_I\ln\upsilon-N_I\ln\upsilon_I+\frac{\bar{\upsilon}_{II}N_I}{\upsilon_I} \tag{A.4.1b}$$

The free energy difference between the solution and the pure components in the isotropic state is called mixing free energy(2).

$$\begin{aligned}\beta\Delta F_{mixing}(N_A,N_I)&=N_A\ln c_A+N_I\ln c_I+N_A\left(WS^2-\ln(I_0)\right)\\&+\bar{\upsilon}_{AA}N_Ac_A\left(1-\frac{5}{8}\left(1-\frac{11}{8}h\right)S^2\right)+2\bar{\upsilon}_{AI}N_Ic_A+\bar{\upsilon}_{II}N_Ic_I+Uc_A\upsilon_A^2N_AS^2+\frac{32\pi^2}{3}\left(\frac{\xi}{p_0}\right)^2\frac{L}{D_{eff}}N_AS^2\\&+N_A\ln\upsilon_A-\frac{\bar{\upsilon}_{AA}N_A}{\upsilon_A}+N_I\ln\upsilon_I-\frac{\bar{\upsilon}_{II}N_I}{\upsilon_I}\end{aligned} \tag{A.4.2}$$

As alluded in subsection 2.1 of the article, υ which is an arbitrary volume, merely plays dimensional consistency not any other role. Herein, one can see that it is included in eqn. (A.4.2).

Given $\phi_i = c_i \upsilon_i$, $N_i = \frac{\phi_i V}{\upsilon_i}$, incompressibility $\phi_A + \phi_I = 1$, small-sized solve $n_I = 1$, and the isotropic Flory-Huggins parameter $\chi = a^3 \left(\frac{2\bar{\upsilon}_{AI}}{\upsilon_A \upsilon_I} - \frac{\bar{\upsilon}_{AA}}{\upsilon_A^2} - \frac{\bar{\upsilon}_{II}}{\upsilon_I^2} \right)$, the Flory-Huggins theory gives eqn. (A.4.3b).

$$\beta \Delta F_{mixing}(N_A, N_I) = N_A \ln \phi_A + N_I \ln \phi_I + 2\bar{\upsilon}_{AI} N_I c_A + \bar{\upsilon}_{II} N_I \left(c_I - \frac{1}{\upsilon_I} \right) + \bar{\upsilon}_{AA} N_A \left(c_A - \frac{1}{\upsilon_A} \right)$$
$$N_A \left(WS^2 - \ln(I_0) \right) + \left(\bar{\upsilon}_{AA} c_A \left(-\frac{5}{8} \left(1 - \frac{11}{8} h \right) \right) + U c_A \upsilon_A^2 + \frac{32\pi^2}{3} \left(\frac{\xi}{p_0} \right)^2 \frac{L}{D_{eff}} \right) N_A S^2 \qquad \text{(A.4.3a)}$$

$$\beta \Delta F_{mixing}(N_A, N_I) = N_T \left(\frac{\phi_A \ln \phi_A}{n_A} + \phi_I \ln \phi_I + \phi_A \phi_I \chi + \frac{\phi_A}{n_A} \left(\frac{1}{2} WS^2 - \ln(I_0) \right) \right) \qquad \text{(A.4.3b)}$$

A.5. Chemical potential in terms of total dimensionless free energy per lattice and volume fraction

In this subsection, we develop the chemical potential for mesogen in the phase j (i.e. Cho or Iso), eqn. (29a). In addition, doing similar mathematical manipulations leads to the chemical potential for the solvent.

Knowing that $F = \frac{\beta F}{N_T}$, we reach to eqn. (A.5.1).

$$\mu_A^j = \left(\frac{\partial F^j}{\partial N_A} \right)_{N_I, T} = \frac{1}{\beta} \left(N_T \left(\frac{\partial F}{\partial N_A} \right)_{N_I, T} + F \left(\frac{\partial N_T}{\partial N_A} \right)_{N_I, T} \right) \qquad \text{(A.5.1)}$$

To determine the $\frac{\partial N_T}{\partial N_A}$, we should use the definition of $N_T = n_A^{eff} N_A + n_I N_I$.

$$\left(\frac{\partial N_T}{\partial N_A} \right)_{N_I, T} = n_A^{eff} \qquad \text{(A.5.2)}$$

Now, we should write the $\left(\frac{\partial F}{\partial N_A} \right)_{N_I, T}$ in term of volume fraction.

$$\left(\frac{\partial F}{\partial N_A} \right)_{N_I, T} = \left(\frac{\partial F}{\partial \phi_A} \right)_{N_I, T} \left(\frac{\partial \phi_A}{\partial N_A} \right)_{N_I, T} \qquad \text{(A.5.3)}$$

The definition of volume fraction with the assumption of equal lattice size is $\phi_A = n_A^{eff} N_A / N_T$, therefore we are now able to determine $\left(\frac{\partial \phi_A}{\partial N_A}\right)_{N_I,T}$.

$$\left(\frac{\partial \phi_A}{\partial N_A}\right)_{N_I,T} = \frac{1}{N_T}\left(n_A^{eff} - \phi_A\left(\frac{\partial N_T}{\partial N_A}\right)_{N_I,T}\right) \tag{A.5.4}$$

Substituting eqn. (A.5.2) to eqn. (A.5.4) gives the desired form of $\left(\frac{\partial \phi_A}{\partial N_A}\right)_{N_I,T}$.

$$\left(\frac{\partial \phi_A}{\partial N_A}\right)_{N_I,T} = \frac{1}{N_T} n_A^{eff} \phi_I \tag{A.5.5}$$

Finally, we should substitute eqns. (A.5.2, A.5.5) to eqn. (A.5.1) to reach the final form that we wanted.

$$\mu_A^j = \left(\frac{\partial F^j}{\partial N_A}\right)_{N_I,T} = n_A^j\left(F^j + \phi_I^j\left(\frac{\partial F^j}{\partial \phi_A^j}\right)_{\phi_I^j,T}\right) \tag{A.5.6}$$

A.6. Functionality of L/D_{eff}

The ionic strength of the dispersion of collagen in an aqueous acetic acid solution is represented by:

$$I = \frac{1}{2}\sum_i m_i Z_i^2 = \frac{1}{2}\sum_i m_i \tag{A.6.1}$$

because the charge number of acetic acid is one, $AA \leftrightarrow A^- + H^+$. Now we formulate the summation of molarities for all mobile ions. Let $N_{H^+}^m$ and $N_{A^-}^m$ are the number of hydronium ions and acetate ions that are mobile in the dispersion. Hence, the total number of mobile ions, N_T^m, is given by

$$N_T^m = N_{H^+}^m + N_{A^-}^m \tag{A.6.2}$$

To determine $N_{A^-}^m$, we shall take into consideration that the number of mobile acetate is the summation of number of existing hydronium ions, N_{H+}^m, and the number of protonated hydrogen that are adsorbed on the collagen backbone, N_{H+}^b. This consideration is due to the principle of charge neutrality, see Fig. 2.

$$N_{A^-}^m = N_{H+}^m + N_{H+}^b \tag{A.6.3}$$

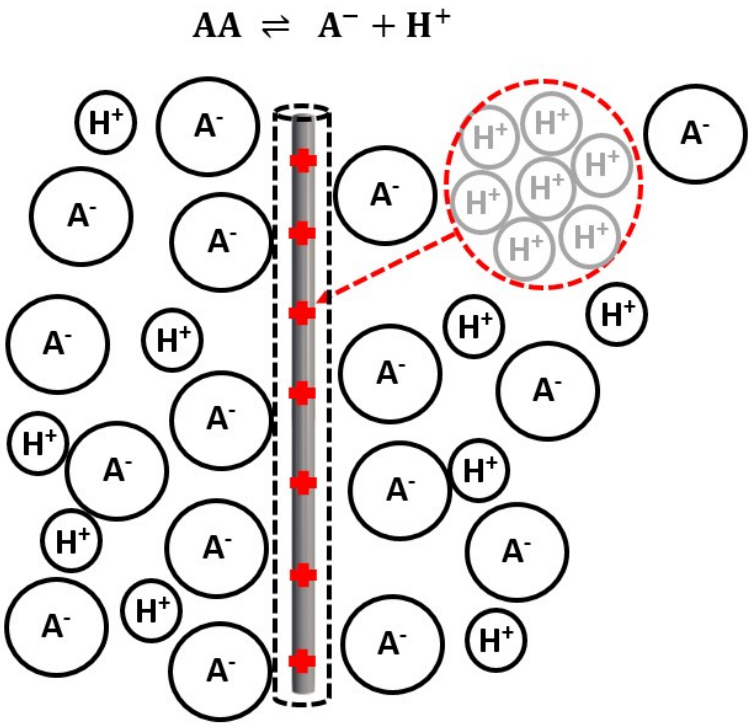

Fig. 2 : Schematic of the principle of charge neutrality. There are 16 H^+ (7 cations on the collagen backbone and 9 cations are mobile in dispersion) and 16 A^-.

The number of protonated hydrogen on the collagen backbone is simply given by $N^b_{H+}=N_A\Lambda(pH)L$. Substituting the eqn. (A.6.3) into eqn. (A.6.2) leads to

$$N^m_T=2N^m_{H^+}+N_A\Lambda(pH)L=2m^m_{H^+}VN_{avo}+m_A\Lambda(pH)LVN_{avo} \tag{A.6.4}$$

Hence, the ionic strength of dispersion can be written in known terms.

$$I=m^m_{H^+}+\frac{1}{2}m_A\Lambda(pH)L \tag{A.6.5}$$

Since $m^m_{H^+}$ shows the molarity of mobile hydronium ions that do not have tendency to absorbed on the collagen backbone anymore, from equilibrium of acetic acid in water, we can conclude that $m^m_{H^+}=\sqrt{k_d[AA]}$ (13).

$$I=\sqrt{k_d[AA]}+\frac{1}{2}m_A\Lambda(pH)L \tag{A.6.6}$$

As discussed later on in Appendix B.2, $\Lambda(pH)$ can be determined by knowing the $m^m_{H^+}$ because $pH=-\log_{10}^{m^m_{H^+}}$ (13).

Now that the functionality of ionic strength, eqn. (A.6.6), is obtained, one can readily conclude that

$$[AA] = \text{constant} \ : \ m_A \uparrow \Rightarrow I \uparrow \Rightarrow \kappa^{-1} \downarrow \Rightarrow \ D_{eff} \downarrow \Rightarrow \ L/D_{eff} \uparrow$$

$$m_A = \text{constant} \ : \ [AA] \uparrow \Rightarrow I \uparrow \Rightarrow \kappa^{-1} \downarrow \Rightarrow \ D_{eff} \downarrow \Rightarrow \ L/D_{eff} \uparrow$$

The trend of variation in the ratio of L/D_{eff} with respect to the concentrations of acid and collagen is shown in Fig. 3.

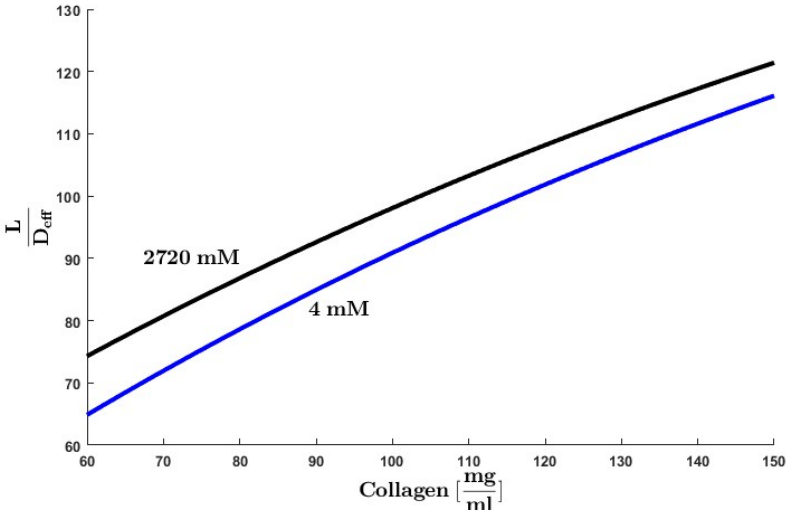

Fig. 3 : Dependence of L/D_{eff} on collagen concentration .

The obtained range of L/D_{eff} is consistent with previous work and data (14).

Appendix B: Model Parameters and Material Properties Used in Computation of Phase Diagrams

In this section, we have first tabulated some physical properties for the components that exist in our study, Table 1 Thereafter, other parameters have been brought to the subsequent subsections for further discussion.

Table 1: The physical properties of components in acidic collagenous solution.

Physical property	**value**	**Reference**
$\rho_{collagen}\left(\frac{g}{l}\right)$	1120	(15)
$Mw_{Collagen}\,(Da)$	285,000	(16)
$D_{Bare}\,(nm)$	1.5	(16)
$L(nm)$	300	(16)
$p_0\,(\mu m)$	2~22 (depending on the concentrations)	(17)
$\delta(nm)$	5~24 (depending on the concentration of collagen)	(18)

It is worth mentioning that, based on the reference (17); the experimental pitch (in unit of μm) for the collagenous solutions can be fitted with respect to collagen concentration (in unit of mg/ml). For solutions prepared in 5mM and 500mM acetic acid, the empirical correlations are respectively given by

$$p_0/2 = 11C^{-0.02} \tag{B.1}$$

$$p_0/2 = 140C^{-0.92} \tag{B.2}$$

For other acetic concentration, we have used the interpolated values. Fig. 4 shows the trend of experimental pitch with respect to variations of collagen concentrations.

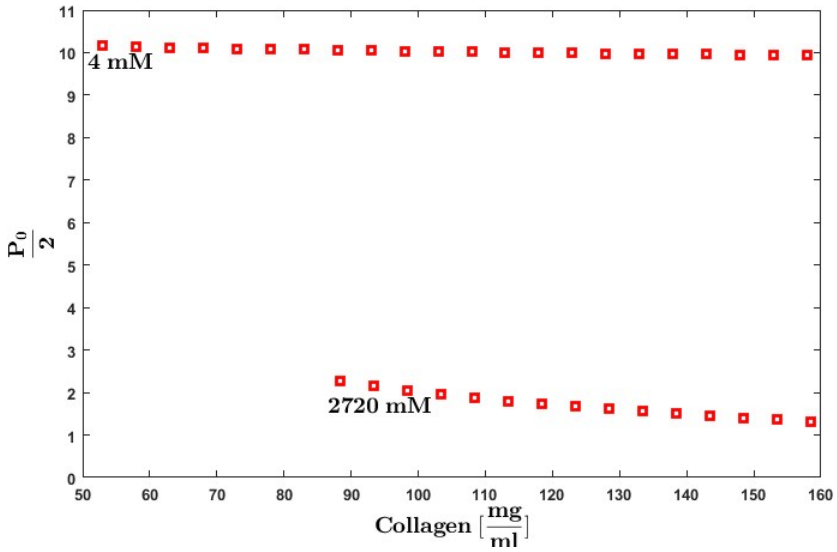

Fig. 4 : Experimental equilibrium pitch extracted from the reference (17).

B.1. Isotropic Flory-Huggins parameter, χ

In this subsection, we aim to provide an acceptable estimation of isotropic Flory-Huggins parameter. Actually, values of parameters in eqn. (27) are not always available; instead, we unavoidably turn to an estimation method. As per regular solution theory, the dimensionless isotropic Flory–Huggins interaction parameter, χ, is estimated using Hansen solubility parameters, eqn. (B.1.1) (19).

$$\chi=\alpha\frac{\upsilon_I}{k_B T}\left(\left(\delta_{A,d}-\delta_{I,d}\right)^2+0.25\left(\delta_{A,p}-\delta_{I,p}\right)^2+0.25\left(\delta_{A,h}-\delta_{I,h}\right)^2\right) \qquad (B.1.1)$$

υ_I stands for volume of solvent, which is isotropic component in present work. $\delta_{i,j}$ is Hansen solubility parameter; the first subscript shows the component which can be either isotropic (I) or anisotropic (A), the second subscript d, p and h are contributions because of dispersive, polar and hydrogen bonding. In addition, α is the experimental fitting parameter bounded between 0 to 1. The solubility parameters for this system are summarized in Table 2 (20).

Table 2: Solubility parameters

Solubility parameters	Values $\left(\frac{J}{cm^3}\right)^{1/2}$
$\delta_{collagen,d}$	16
$\delta_{collagen,h}$	23.6
$\delta_{collagen,p}$	20.3
$\delta_{water,d}$	12.2
$\delta_{water,h}$	37.3
$\delta_{water,p}$	27.3
$\delta_{acetic\ acid,d}$	15.4
$\delta_{acetic\ acid,h}$	15.2
$\delta_{acetic\ acid,p}$	9.4
$\delta_{collagen,d}$	16

α has not been documented for collagen. We have unavoidably used experimental value of mesogen with molecules similar to collagen molecules. We have then chosen cellulose acetate because its Flory-Huggins parameter in the dilute solution has reported 0.4 (21). The solvent mainly consists of water molecules, thus we took the radius of solvent as 1.4 Å. Finally, substitution of these physical values into eqn. (B.1.1) leads to following estimation for the dimensionless isotropic Flory-Huggins interaction.

$$\chi > \frac{120}{T(K)} \qquad (B.1.2)$$

(K) shows that the temperature must be absolute in unit of Kelvin.

B.2. The pH-dependent linear charge density of collagen

The aim of this subsection is to present an acceptable method to determine the linear charge density of tropocollagen in various pH because the linear charge density is required in eqn. (2b).

Type I collagen is composed of three helical polypeptide chains; two α1(I) chains and one α2(I). Each chain contains roughly1052 amino acid residues twisted around each other in the form of a right-handed triple helix. Collagen has the repeating triplets of sequence Gly-X-Y where X and Y are often proline (~28%) and hydroxyproline (~38%) residues, respectively(16).

In our study, we have focused on the acidic collagenous solutions because the rods are far away from fibrogenesis and the primary architecture of collagenous plywood are formed. In the acidic pHs, the amine functional groups are protonated, and as a result the rods become positively charged (Fig. 5 indicates the linear charge density of collagen Type I against the pH). The eqn. (2b) of the article requires the linear charge density of collagen. One approximate but good method to determination of a peptide charge is as follows. We should compare the pK_a of each residues with the pH of solution. If pK_a is greater and pH, that residue gets protonated, otherwise deprotonated. This procedure can readily be done using a protein calculator(22). Additionally, we have used UniProt Knowledgebase (23) to obtain the sequence of rat tail; rat CO1A1: P02454; rat CO1A2: P02466.

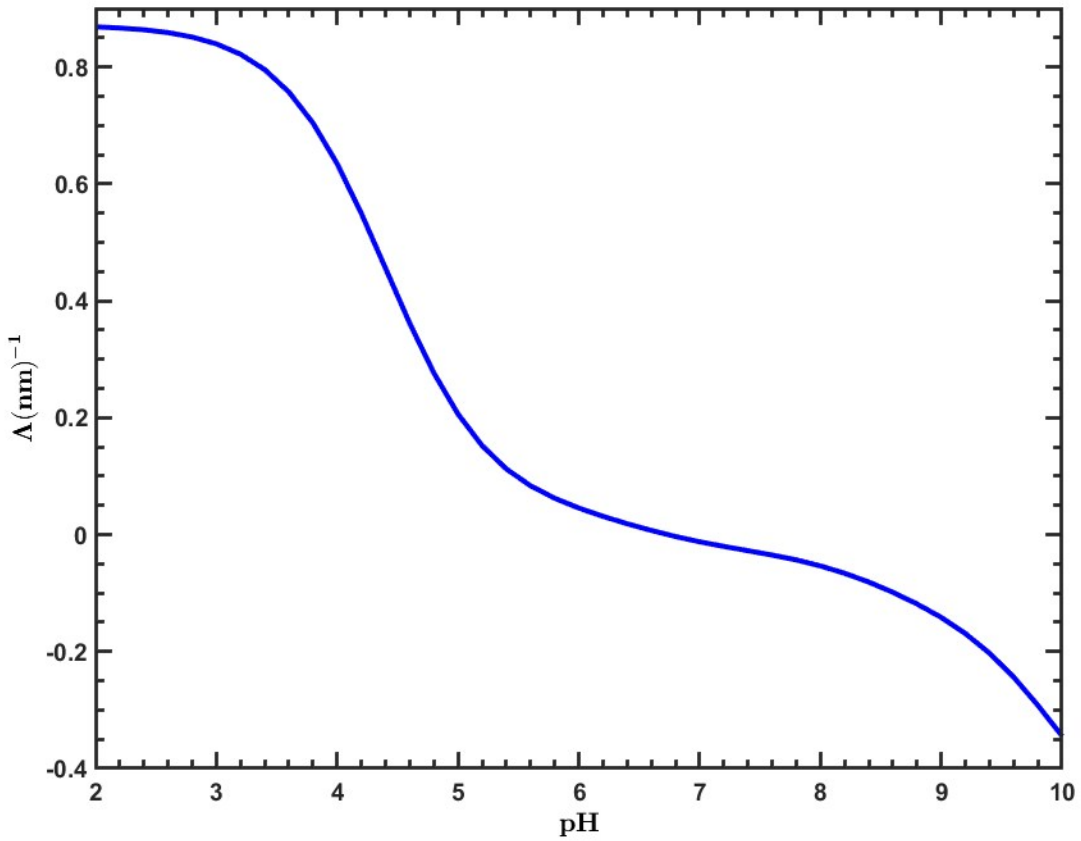

Fig. 5 : The pH-dependent linear charge density of collagen.

The minimum distance between fixed charges on the backbone of a polyelectrolyte cannot be less than the Bjerrum length, which is about λ_B =0.79 nm in our study (6). Based on the assumption of uniform charge distribution, Fig. 5 satisfies the mentioned physical constraint because the averaged distance between charges is $L/(|\Lambda|L-1)>1nm>\lambda_B$.

Appendix C: Consistency with previous studies

In this section, we show that our suggested model (eqns.(3,26)) can be reduced to the other well-established models if some of the mechanisms are ignored.

C.1. Onsager Model

Under condition that the solution is only comprised of rigid rodlike uncharged mesogens; the main mechanisms become the translational and orientational entropies along with the excluded

volume. In eqn. (3), if we consider $M(\psi(\mathbf{u}))=C(\psi(\mathbf{u}))=0$, we reach to the energy landscape proposed by Onsager (24).

C.2. Matsuyama et al. Model (ref(2))

The general structure of the energy landscape developed in this study is based on Matsuyama et al. model (2) (comparing eqn. (3.6) of the mentioned reference with eqn. (26) in our work). The main difference between our suggested theory and Matsuyama et al. is that, due to the nature of the acidic collagenous solutions, we have also included the mechanisms of chirality and interchain electrostatic (i.e. repulsion and twisting). Here, we aim to show that our proposed theory can be simplified to the Matsuyama et al. theory that has been used in other studies (7, 8, 25, 26). Giving that the included mechanisms are negligible therefore we should consider the $U^{elc}=h=\kappa^{-1}=0$ and $p_0=\infty$. Doing so, the net cholesteric potential ends up like eqn. (C.2.1a,b).

$$W=\phi_A \frac{L}{D}\left(\frac{5}{4}+\chi_a\right) \tag{C.2.1a}$$

$$\chi_a=\frac{\pi}{2}D^3\beta U^{MS} \tag{C.2.1b}$$

Considering our suggested model with the net potential given by eqn. (C.2.1a,b) leads to eqn. (3.6) of reference (2).

Appendix D: Nomenclature

Table 3: Nomenclature

Symbol	Units	Definition
a^3	m^3	volume of each lattice unit
$B_2(\psi(\mathbf{u}))$	[-]	excluded volume based on the second virial approximation
$C(\psi(\mathbf{u}))$	[-]	geometric chirality of mesogen
c'_A	[-]	dimensionless number density
c_A	m^{-3}	number density
D_{eff}	m	effective diameter

Symbol	Units	Definition
D	m	bare diameter
$d\Omega$	radian	solid angle
E^{MS}	j	Energy due to Maier-Saupe contribution (i.e. attractive interaction)
E^{elc}	j	Energy due to interchain electrostatic interactions (i.e. repulsion and twisting)
$E^{Cholesteric}$	j	Energy due to Frank distorsion (i.e. cholesteric)
Ei	[-]	exponential integral
F^{s}	j	free energy of solution
h	[-]	magnitude of the twisting effect
$\mathbf{h}$	[-]	helix unit vector
I	molar	ionic strength,
k_B	$m^2.kg.s^{-2}.K^{-1}$	Boltzmann constant, $1.38064852 \times 10^{-23}$
L	m	contour length
L_l	j/m	elastic constant
$M(\psi(\mathbf{u}))$	[-]	the orientation-dependent intermolecular interactions
m_i	molar	molar concentration of i^{th} mobile ion
N_{avo}	mol^{-1}	Avogadro's number, $6.022140857 \times 10^{23}$
N_A and N_I	[-]	number of chiral mesogens and isotropic component
N_T	[-]	total number of lattice site
$N^{m}_{H^+}$	[-]	number of hydronium ions
$N^{m}_{A^-}$	[-]	number of acetate ions
N^{m}_{T}	[-]	total number of mobile ions
N^{b}_{H+}	[-]	number of protonated hydrogen that are adsorbed on the collagen backbone
n^{eff}_{A}	[-]	number of segments on the backbone of

Symbol	Units	Definition
		mesogen
$\mathbf{n}$	[-]	uniaxial direction
p_0	m	pitch
$P_2(\mathbf{u}\cdot\mathbf{n})$	[-]	second Legendre polynomial of angle between the macromolecule and uniaxial direction (i.e. local order parameter)
q	m^{-1}	pitch wave
$\mathbf{Q}$	[-]	quadrupole moment tensor, well-known as **Q**-tensor
S	[-]	macroscopic uniaxial order parameter
U	$j.m^{-3}$	potential of orientation-dependent intermolecular interaction
U_i^{MS}	j	one-body mean field potential of i^{th} rod for attractive interactions on the other existing rods in the system
U'^{MS}	$j.m^{-3}$	positive constant independent of temperature related to Maier-Saupe parameter
U^{MS}	$j.m^{-3}$	positive constant independent of temperature, Maier-Saupe parameter
U_i^{elc}	j	one-body mean field potential of i^{th} rod for electrostatic interactions (i.e. repulsion and twisting) on the other existing rods in the system
U'^{elc}	$j.m^{-3}$	strength of electrostatic potential (i.e. repulsion and twisting)
U^{elc}	$j.m^{-3}$	strength of electrostatic interaction among the rods (i.e. repulsion and twisting)
$\mathbf{u}$ and $\mathbf{u}'$	[-]	The orientations of two rod-like macromolecules
V	m^3	volume of system
W	[-]	net cholesteric potential
z	m	z-component of space
Z	[-]	coordination number

Symbol	Units	Definition
Z_i	[-]	charge number of i^{th} mobile ion
α	[-]	double-layer thickness parameter
β	j^{-1}	thermal energy
γ	radian	angle between the rods
γ_E	[-]	Euler constant, 0.5772
$\boldsymbol{\delta}$	[-]	Kronecker delta
$\delta_{i,j}$	$(j.m^{-3})^{1/2}$	solubility parameters, i indicates the substance and j stands for the kind of bonding. j can be d, p and h which are for dispersive, polar and hydrogen bonding, respectively.
ΔS_O	[-]	orientational entropy
η' and η	[-]	constants determined by normalization of distribution function
θ	radian	polar angle
κ^{-1}	m	Debye screening length
λ_B	m	Bjerrum length
λ_{ChE}	[-]	coupling parameters of chirality-electrostatic
λ_{ExE}	[-]	coupling parameters of excluded volume-electrostatic
λ_{II}	[-]	coupling parameters of intermolecular interaction
Λ	charge number per meter	linear charge density
μ^o	j	standard particle chemical potential
ξ	m	coherence length or correlation length
$\sigma\left(\psi\left(\mathbf{u}\right)\right)$	[-]	effect of orientational entropy
$\bar{\upsilon}_{AA}$, $\bar{\upsilon}_{IA}$ and $\bar{\upsilon}_{II}$	m^3	average excluded-volume between mesogen-mesogen, mesogen-isotropic component and isotropic component- isotropic component.

Symbol	Units	Definition
υ_A and υ_I	m^3	molecular volumes of mesogen and isotropic component
υ	m^3	volume scale, an arbitrary volume
φ	radian	azimuthal angle
ϕ_A^{eff} and ϕ_I^{eff}	[-]	effective volume fraction of mesogen and isotropic component
χ	[-]	isotropic Flory-Huggins parameter
$\psi(\mathbf{u})$	[-]	single-rod orientational distribution function
F	[-]	total dimensionless free energy per lattice site

References

1. Drwenski T, Dussi S, Hermes M, Dijkstra M, Roij Rv. Phase diagrams of charged colloidal rods: Can a uniaxial charge distribution break chiral symmetry? 2016;144(9):094901.
2. Matsuyama A, Kato T. Theory of binary mixtures of a flexible polymer and a liquid crystal. J Chem Phys. 1996;105(4):1654-60.
3. Lin-Liu YR, Shih YM, Woo C-W. Molecular theory of cholesteric liquid crystals and cholesteric mixtures. Physical Review A. 1977;15(6):2550-7.
4. Maier W, Saupe AJZfNA. Eine einfache molekular-statistische Theorie der nematischen kristallinflüssigen Phase. Teil l1. 1959;14(10):882-9.
5. Maier W, Saupe AJZfNA. Eine einfache molekular-statistische Theorie der nematischen kristallinflüssigen Phase. Teil II. 1960;15(4):287-92.
6. Doi M. Soft Matter Physics: OUP Oxford; 2013.
7. Das SK, Rey AD. Texture formation under phase ordering and phase separation in polymer-liquid crystal mixtures. J Chem Phys. 2004;121(19):9733-43.
8. Gurevich S, Soule E, Rey A, Reven L, Provatas N. Self-assembly via branching morphologies in nematic liquid-crystal nanocomposites. Physical Review E. 2014;90(2).
9. De Luca G, Rey AD. Chiral front propagation in liquid-crystalline materials: Formation of the planar monodomain twisted plywood architecture of biological fibrous composites. Physical review E, Statistical, nonlinear, and soft matter physics. 2004;69(1 Pt 1):011706.
10. Muševič I. Liquid Crystal Colloids: Springer International Publishing; 2017.
11. Sagan H. Introduction to the Calculus of Variations: McGraw-Hill; 1969.
12. Matsuyama A. Phase separations in mixtures of a liquid crystal and a nanocolloidal particle. The Journal of Chemical Physics. 2009;131(20):204904.
13. Silberberg M. Chemistry: The Molecular Nature of Matter and Change: McGraw-Hill; 2006.
14. Gutierrez OFA, Rey AD. Theory and Simulation of Cholesteric Film Formation Flows of Dilute Collagen Solutions. Langmuir. 2016;32(45):11799-812.

15. Cusack S, Miller A. Determination of the elastic constants of collagen by Brillouin light scattering. Journal of Molecular Biology. 1979;135(1):39-51.
16. Voet D, Voet JG. Biochemistry. Hoboken, NJ: John Wiley & Sons; 2011.
17. Peixoto PD, Deniset-Besseau A, Schanne-Klein MC, Mosser G. Quantitative assessment of collagen I liquid crystal organizations: role of ionic force and acidic solvent, and evidence of new phases. Soft Matter. 2011;7(23):11203-10.
18. Gobeaux F, Belamie E, Mosser G, Davidson P, Panine P, Giraud-Guille MM. Cooperative Ordering of Collagen Triple Helices in the Dense State. Langmuir. 2007;23(11):6411-7.
19. Lindvig T, Michelsen ML, Kontogeorgis GM. A Flory–Huggins model based on the Hansen solubility parameters. Fluid Phase Equilibria. 2002;203(1):247-60.
20. Miller RG, Bowles CQ, Chappelow CC, Eick JD. Application of solubility parameter theory to dentin-bonding systems and adhesive strength correlations. 1998;41(2):237-43.
21. Mark JE. Physical Properties of Polymers Handbook: Springer New York; 2007.
22. v3.4 PC. pH-dependent Linear Charge Density 2013 [Available from: http://protcalc.sourceforge.net/.
23. Knowledgebase U. Amino Acids Sequence 2018 [Available from: https://www.uniprot.org/.
24. Odijk T. Theory of lyotropic polymer liquid crystals. Macromolecules. 1986;19(9):2313-29.
25. Susanta KD, Alejandro DR. Computational modelling of multiscale morphologies in polymer–liquid crystal blends. Nanotechnology. 2005;16(7):S330.
26. Das SK, Rey AD. Computational modelling of multi-phase equilibria of mesogenic mixtures. Computational Materials Science. 2004;29(2):152-64.